Proceedings of the 17th World Congress
The International Federation of Automatic Control
Seoul, Korea, July 6-11, 2008

Sampling of noisy signals: spectral vs anti-aliasing filters ⋆

Marian J. Błachuta * **and Rafał T. Grygiel** *

* *Department of Automatic Control, The Silesian University of Technology, 16 Akademicka St., PL44-101, Gliwice, Poland (e-mail: marian.blachuta@polsl.pl, rafal.grygiel@polsl.pl)*

Abstract:
In the paper we study the properties of sampling stochastic signals corrupted by a wide-band stochastic noise where samples are taken either directly from resulting signal, or as the output from a continuous-time filter. We consider two types of filters: anti-aliasing filters whose characteristics depend solely on sampling period, and Kalman filters, whose characteristics depend on spectra of signals of interest. We also study possible improvement attained by discrete-time Kalman filtering applied to the sampled signal. We compare the results of two competitive methods: classical point-wise sampling followed by discrete-time filtering, and continuous-time filtering prior to sampling possibly followed by digital filtering. The study is performed for a wide range of sampling periods and noise-to-signal ratios and leads to important practical conclusions.

1. INTRODUCTION

In scientific literature Feuer & Goodwin (1996); Wittenmark et al. (2002); Åström & Wittenmark (1997) strong belief is expressed that additional analog elements in the form of so called anti-aliasing filters are necessary to guarantee correct sampling for further digital signal processing. Although various solutions are possible, these filters usually take the form of Butterworth filters whose cutoff frequency equals to the so called Nyquist frequency $\omega_N = \pi/h$ depending solely on sampling period h.

This belief is usually supported by informal speculations based on Shannon-Kotelnikov Reconstruction Theorem, e.g. Jerri (1977), which states that in order to reconstruct the signal $s(t)$ from its samples $s(ih), -\infty < i < \infty$, the sampling frequency should be twice the highest frequency component in the signal. Since the spectra of physical signals often stretch on infinite frequency range, this gives rise to the idea of filters that cut off the portion of frequency spectrum lying outside the region determined by that theorem. These portions cause the effect of frequency folding responsible for the spectrum of a sampled process to differ from its continuous-time original, see Fig. 1. Anti-aliasing filters prevent the spectrum from folding, which is supposed to be necessary.

We do not share this view since the only effect of anti-aliasing filter is deformation of the signal to be sampled, such that its reconstruction, although theoretically possible, differs from the original, see Fig. 2 for an example. This idea, however, makes sense when the signal $s(t)$ is contaminated with a wide-band noise $n(t)$, and we are interested in reconstructing samples $s(ih)$ of the original signal $s(t)$ from samples $y(ih)$ of $y(t) = s(t)+n(t)$, see Fig.

⋆ This work has been granted by the Polish Ministry of Science and Higher Education from funds for years 2008-2011

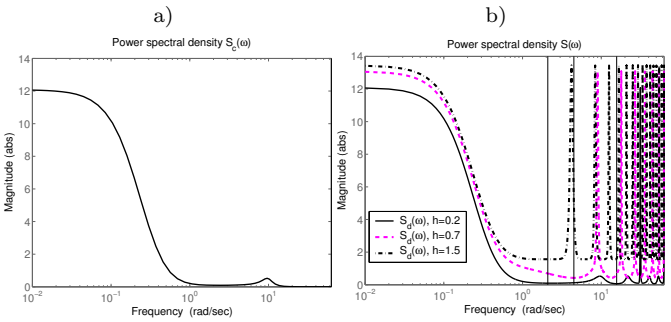

Fig. 1. Spectral densities: $S_c(\omega)$ for $y(t)$; $S_d(\omega)$ for $y(ih)$

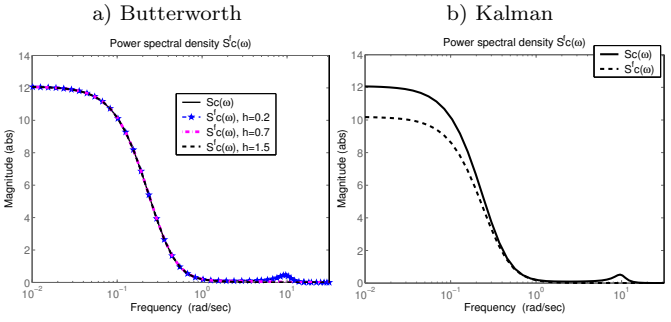

Fig. 2. $S_c(\omega)$, and $S_c^f(\omega)$ of original and filtered signals

3. In this case putting an appropriate analog filter between the source of $y(t)$ and the sampler might be justified.

We claim that such filter should depend on the spectral characteristics of both $s(t)$ and $n(t)$ rather than on sampling frequency. In contrast to anti-aliasing filter we will call it a spectral filter.

We also show that in either case anti-aliasing filter makes little or no sense except for certain sampling periods for which the properties of an anti-aliasing filter approach that of a properly designed spectral filter.

These claims will be proved by quantitative analysis of both filtration and sampling problems, and of combinations of them.

2. PROBLEM FORMALIZATION

A model of signal contaminated by noise presented in Fig. 3a) consists of two forming filters represented by transfer functions $K_s(s)$ and $K_n(s)$ driven by white noise signals $\dot{\xi}_s(t)$ and $\dot{\xi}_n(t)$. Further analysis is based on state-space methods, therefore state-space description of this model is required.

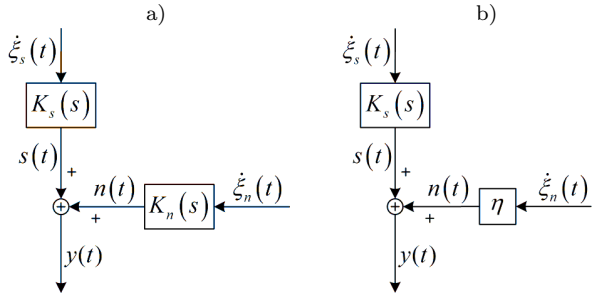

Fig. 3. a) Model of signal contaminated by noise, b) Simplified model with white noise

2.1 State-space model of signal contaminated by noise

To analyse the properties of sampling we will use state-space models of the system in Fig.3 consisting of signal

$$\dot{\boldsymbol{x}}_s(t) = \boldsymbol{A}_s\boldsymbol{x}_s(t) + \boldsymbol{c}_s\dot{\xi}_s(t), \tag{1}$$
$$s(t) = \boldsymbol{d}_s'\boldsymbol{x}_s(t), \tag{2}$$

and noise model

$$\dot{\boldsymbol{x}}_n(t) = \boldsymbol{A}_n\boldsymbol{x}_n(t) + \boldsymbol{c}_n\dot{\xi}_n(t), \tag{3}$$
$$n(t) = \boldsymbol{d}_n'\boldsymbol{x}_n(t). \tag{4}$$

where $\dim \boldsymbol{x}_s = n_s$, $\dim \boldsymbol{x}_n = n_n$, $\boldsymbol{x}_s(t)$, $\boldsymbol{x}_n(t)$ are state vectors, $\boldsymbol{A}_s$, $\boldsymbol{A}_n$ are matrices, $\boldsymbol{c}_s$, $\boldsymbol{c}_n$, $\boldsymbol{d}_s$, and $\boldsymbol{d}_n$ are vectors of appropriate dimensions. The initial conditions $\boldsymbol{x}_s(0)$ and $\boldsymbol{x}_n(0)$ are assumed to be a normal random vectors, $\boldsymbol{x}_s(0) \sim \mathcal{N}(\boldsymbol{0}, \boldsymbol{Q}_{s,0})$, $\boldsymbol{x}_n(0) \sim \mathcal{N}(\boldsymbol{0}, \boldsymbol{Q}_{n,0})$. Processes $\dot{\xi}_s(t)$ and $\dot{\xi}_s(t)$ are independent continuous-time white noises with zero means and covariance functions defined as unit Dirac pulse functions, i.e.:

$$\mathrm{E}\left[\dot{\xi}_s(t)\right] = 0, \qquad \mathrm{E}\left[\dot{\xi}_s(t)\dot{\xi}_s(\tau)\right] = \delta(t-\tau); \tag{5}$$
$$\mathrm{E}\left[\dot{\xi}_n(t)\right] = 0, \qquad \mathrm{E}\left[\dot{\xi}_n(t)\dot{\xi}_n(\tau)\right] = \delta(t-\tau). \tag{6}$$

The disturbed signal $y(t)$ is the sum of the signal of interest $s(t)$ and noise $n(t)$:

$$y(t) = s(t) + n(t) \tag{7}$$

System (1)-(4) with (7) can be aggregated to:

$$\dot{\boldsymbol{x}}(t) = \boldsymbol{A}\boldsymbol{x}(t) + \boldsymbol{C}\dot{\boldsymbol{\xi}}(t), \tag{8}$$
$$s(t) = \boldsymbol{d}_0'\boldsymbol{x}(t), \tag{9}$$
$$y(t) = \boldsymbol{d}'\boldsymbol{x}(t), \tag{10}$$

where:

$$\boldsymbol{A} = \begin{bmatrix} \boldsymbol{A}_s & \boldsymbol{0} \\ \boldsymbol{0} & \boldsymbol{A}_n \end{bmatrix}, \quad \boldsymbol{C} = \begin{bmatrix} \boldsymbol{c}_s & \boldsymbol{0} \\ \boldsymbol{0} & \boldsymbol{c}_n \end{bmatrix}, \quad \boldsymbol{d}_0 = \begin{bmatrix} \boldsymbol{d}_s \\ \boldsymbol{0} \end{bmatrix},$$
$$\boldsymbol{d} = \begin{bmatrix} \boldsymbol{d}_s \\ \boldsymbol{d}_n \end{bmatrix}, \quad \boldsymbol{x}(t) = \begin{bmatrix} \boldsymbol{x}_s(t) \\ \boldsymbol{x}_n(t) \end{bmatrix}, \quad \dot{\boldsymbol{\xi}}(t) = \begin{bmatrix} \dot{\xi}_s(t) \\ \dot{\xi}_n(t) \end{bmatrix}$$

2.2 Continuous-Time Filters

Representatives of two sort continuous filters are investigated in this paper: Butterworth filter as an anti-aliasing filter and Kalman filter as a spectral one.

Continuous-time Butterworth filter Transfer function of Butterworth filter has the form:

$$K^{fa}(s) = \frac{1}{B_n\left(\frac{s}{\omega_o}\right)}, \tag{11}$$

where $B_n(*)$ is the n-th degree Butterworth's polynomial and ω_o is called the cutoff frequency. In this paper ω_o will be assumed as Nyquist frequency $\omega_o = \omega_N = \frac{\pi}{h}$. The first Butterworth's polynomials are definded as follows:

$$B_1(x) = x + 1; \quad B_2(x) = x^2 + \sqrt{2}\cdot x + 1. \tag{12}$$

Continuous-time Kalman filter Since there is no noise in output $y(t)$, the classical Kalman filter for system in (8)–(10)becomes singular. One way to overcome the problem is to assume that white noise $\nu(t)$ with very small spectral density η^2 is add to the output [1], i.e. the output equation instead of (10) becomes:

$$y(t) = \boldsymbol{d}'\boldsymbol{x}(t) + \nu(t), \tag{13}$$

Then the steady-state continuous-time Kalman filter is defined by:

$$\dot{\hat{\boldsymbol{x}}}(t) = \boldsymbol{A}\hat{\boldsymbol{x}}(t) + \boldsymbol{k}_c^f\left[y(t) - \boldsymbol{d}'\hat{\boldsymbol{x}}(t)\right] \tag{14}$$

with:

$$\boldsymbol{k}_c^f = \frac{\boldsymbol{P}\boldsymbol{d}}{\eta^2}; \quad \boldsymbol{A}\boldsymbol{P} + \boldsymbol{P}\boldsymbol{A}' - \frac{\boldsymbol{P}\boldsymbol{d}\boldsymbol{d}'\boldsymbol{P}}{\eta^2} + \boldsymbol{C}\boldsymbol{C}' = 0 \tag{15}$$

The filtered value $\hat{s}(t)$ of $s(t)$ is determined by

$$\hat{s}(t) = \boldsymbol{d}_0'\hat{\boldsymbol{x}}(t). \tag{16}$$

2.3 State-space model of system with analog filter

Either filter, anti-aliasing or Kalman [2], can be expressed in the following form

$$\dot{\boldsymbol{x}}^f(t) = \boldsymbol{A}^f\boldsymbol{x}^f(t) + \boldsymbol{b}^f y(t), \tag{17}$$
$$y^f(t) = \boldsymbol{d}^{f\prime}\boldsymbol{x}^f(t), \tag{18}$$

Then the system consisting of a filter in (17)–(18), together with signal and noise models of (8)-(10) can be aggregated to the following

$$\dot{\boldsymbol{x}}^o(t) = \boldsymbol{A}^o\boldsymbol{x}^o(t) + \boldsymbol{C}^o\dot{\boldsymbol{\xi}}^o(t), \tag{19}$$
$$s(t) = \boldsymbol{d}_s^{o\prime}\boldsymbol{x}^o(t), \tag{20}$$
$$y(t) = \boldsymbol{d}_y^{o\prime}\boldsymbol{x}^o(t), \tag{21}$$
$$y^f(t) = \boldsymbol{d}^{o\prime}\boldsymbol{x}^o(t), \tag{22}$$

[1] unfortunately, when the value of η is too small, then computing $\boldsymbol{P}$ from (15) is problematic; a better choice is to replace the continuous-time filter with a discrete-time one working at sampling frequency high enough. The output of such filter could be resampled at lower frequency if necessary. An alternative solution is to use an approximate continuous-time filter with $\boldsymbol{k}_c^f = \boldsymbol{k}^f/h$.

[2] Superscript 'f' marks generally filter. Superscript 'fa' stands for anti-aliasing filter, while 'fs' stands for a spectral filer.

where:

$$\boldsymbol{A}^o = \begin{bmatrix} \boldsymbol{A}_s & \boldsymbol{0} & \boldsymbol{0} \\ \boldsymbol{0} & \boldsymbol{A}_n & \boldsymbol{0} \\ \boldsymbol{b}^f \boldsymbol{d}_s' & \boldsymbol{b}^f \boldsymbol{d}_n' & \boldsymbol{A}^f \end{bmatrix}, \quad \boldsymbol{C}^o = \begin{bmatrix} \boldsymbol{c}_s & \boldsymbol{0} \\ \boldsymbol{0} & \boldsymbol{c}_n \\ \boldsymbol{0} & \boldsymbol{0} \end{bmatrix},$$

$$\boldsymbol{d}_s^o = \begin{bmatrix} \boldsymbol{d}_s \\ \boldsymbol{0} \\ \boldsymbol{0} \end{bmatrix}, \quad \boldsymbol{d}_y^o = \begin{bmatrix} \boldsymbol{d}_s \\ \boldsymbol{d}_n \\ \boldsymbol{0} \end{bmatrix}, \quad \boldsymbol{d}^o = \begin{bmatrix} \boldsymbol{0} \\ \boldsymbol{0} \\ \boldsymbol{d}^f \end{bmatrix},$$

$$\boldsymbol{x}^o(t) = \begin{bmatrix} \boldsymbol{x}_s(t) \\ \boldsymbol{x}_n(t) \\ \boldsymbol{x}^f(t) \end{bmatrix}, \quad \dot{\boldsymbol{\xi}}^o(t) = \begin{bmatrix} \dot{\xi}_s(t) \\ \dot{\xi}_n(t) \end{bmatrix}$$

2.4 Instantaneous sampling

Assume that the output $y^f(t)$ of the system is sampled at discrete time instants $t_i = ih, i = 0, 1, \ldots$. Then the system is described at sampling points ih by the following discrete-time system:

$$\boldsymbol{x}_{i+1}^o = \boldsymbol{F}^o \boldsymbol{x}_i^o + \boldsymbol{w}_i^o, \tag{23}$$

$$z_i = \boldsymbol{d}^{o\prime} \boldsymbol{x}_i^o, \tag{24}$$

where $\boldsymbol{w}_i^o$ is a zero mean vector Gaussian noise with $\mathrm{E}\{\boldsymbol{w}_i^o \boldsymbol{w}_i^{o\prime}\} = \boldsymbol{W}^o$,

$$\boldsymbol{W}^o = \int_0^h \mathrm{e}^{\boldsymbol{A}^o s} \boldsymbol{C}^o \boldsymbol{C}^{o\prime} \mathrm{e}^{\boldsymbol{A}^{o\prime} s} \, ds \quad \text{and} \quad \boldsymbol{F}^o = \mathrm{e}^{\boldsymbol{A}^o \tau}. \tag{25}$$

Vectors $\boldsymbol{x}_0^o$ and $[\boldsymbol{w}_i^{o\prime}, n_i^o]$ are independent for all $i \geq 0$.

2.5 Discrete-time Kalman filter

The best estimate $\hat{s}_i = E\{s_i | z_i\}$ given samples z_i, $i = 0, 1, \ldots$ is provided [3] by classical discrete Kalman filter in the following form:

$$\hat{\boldsymbol{x}}_{i+1|i+1} = \boldsymbol{F}^m \hat{\boldsymbol{x}}_{i|i} + \boldsymbol{k}^f (z_{i+1} - \boldsymbol{d}^{m\prime} \boldsymbol{F}^m \hat{\boldsymbol{x}}_{i|i}), \tag{26}$$

$$\boldsymbol{k}^f = \frac{\boldsymbol{\Sigma} \boldsymbol{d}^m}{\boldsymbol{d}^{m\prime} \boldsymbol{\Sigma} \boldsymbol{d}^m}, \tag{27}$$

$$\boldsymbol{\Sigma} = \boldsymbol{W}^m + \boldsymbol{F}^m \left(\boldsymbol{\Sigma} - \frac{\boldsymbol{\Sigma} \boldsymbol{d}^m \boldsymbol{d}^{m\prime} \boldsymbol{\Sigma}'}{\boldsymbol{d}^{m\prime} \boldsymbol{\Sigma} \boldsymbol{d}^m} \right) \boldsymbol{F}^{m\prime}. \tag{28}$$

3. SIMPLIFIED MODELS

3.1 Continuous-time model

Very often the power spectrum $S_n(\omega)$ of noise $n(t)$ defined by equations (3)-(4), or by transfer function $K_n(s)$, is much wider than that of the signal of interest $s(t)$. In such case it can be modeled as white noise $n(t)$

$$\mathrm{E}[n(t)] = 0, \qquad \mathrm{E}[n(t) n(\tau)] = \eta^2 \delta(t - \tau); \tag{29}$$

with constant spectral density η^2 independent of frequency ω. The model in (8)-(10) simplifies to

$$\dot{\boldsymbol{x}}_s(t) = \boldsymbol{A}_s \boldsymbol{x}_s(t) + \boldsymbol{c}_s \dot{\xi}_s(t), \tag{30}$$

$$y(t) = \boldsymbol{d}_s' \boldsymbol{x}_s(t) + \eta \dot{\xi}_n(t), \tag{31}$$

$$s(t) = \boldsymbol{d}_s' \boldsymbol{x}_s(t) \tag{32}$$

and the model presented in Fig. 3 simplifies to that of Fig. 3b), with

$$\eta = |K_n(0)| = |\boldsymbol{d}_n' \boldsymbol{A}_n^{-1} \boldsymbol{c}_n| \tag{33}$$

[3] assuming i large enough

The continuous-time Kalman filter is then defined by:

$$\dot{\hat{\boldsymbol{x}}}(t) = \boldsymbol{A}_s \hat{\boldsymbol{x}}(t) + \boldsymbol{k}_c^f \left[y(t) - \boldsymbol{d}_s' \hat{\boldsymbol{x}}(t) \right] \tag{34}$$

with:

$$\boldsymbol{k}_c^f = \frac{\boldsymbol{P} \boldsymbol{d}_s}{\eta^2}; \quad \boldsymbol{A}_s \boldsymbol{P} + \boldsymbol{P} \boldsymbol{A}_s' - \frac{\boldsymbol{P} \boldsymbol{d}_s \boldsymbol{d}_s' \boldsymbol{P}}{\eta^2} + \boldsymbol{c}_s \boldsymbol{c}_s' = 0 \tag{35}$$

The filtered value $\hat{s}(t)$ of $s(t)$ is determined by

$$\hat{s}(t) = \boldsymbol{d}_s' \hat{\boldsymbol{x}}(t) \tag{36}$$

Since only a rough characterization of noise is required, and filter equations are of lower order, this greatly simplifies analog filtering.

Comparison of exact and simplified Kalman filter for an example is shown in Fig. 4 displaying the standard deviation of filtration error $\Delta s' = s(t) - \hat{s}(t)$.

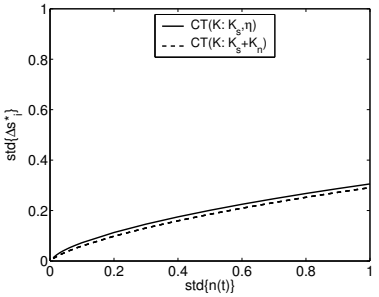

Fig. 4. Comparison of exact and approximate continuous-time Kalman filter – CT(K)

3.2 Simplified continuous-time model with filter

Assume that signal corrupted by noise is modeled by (30)–(32) instead of (8)-(10), and that an analog filter is present. Then equations (19)–(22) simplify to

$$\dot{\boldsymbol{x}}^m(t) = \boldsymbol{A}^m \boldsymbol{x}^m(t) + \boldsymbol{C}^m \dot{\boldsymbol{\xi}}^m(t), \tag{37}$$

$$s(t) = \boldsymbol{d}_s^{m\prime} \boldsymbol{x}^m(t), \tag{38}$$

$$y^f(t) = \boldsymbol{d}^{m\prime} \boldsymbol{x}^m(t), \tag{39}$$

with the initial condition $\boldsymbol{x}^m(0) \sim \mathcal{N}(\boldsymbol{0}, \boldsymbol{Q}_0^m)$ and:

$$\boldsymbol{A}^m = \begin{bmatrix} \boldsymbol{A}_s & \boldsymbol{0} \\ \boldsymbol{b}^f \boldsymbol{d}_s' & \boldsymbol{A}^f \end{bmatrix}, \quad \boldsymbol{C}^m = \begin{bmatrix} \boldsymbol{c}_s & \boldsymbol{0} \\ \boldsymbol{0} & \boldsymbol{b}^f \eta \end{bmatrix}, \quad \boldsymbol{d}_s^m = \begin{bmatrix} \boldsymbol{d}_s \\ \boldsymbol{0} \end{bmatrix},$$

$$\boldsymbol{d}^m = \begin{bmatrix} \boldsymbol{0} \\ \boldsymbol{d}^f \end{bmatrix}, \quad \boldsymbol{x}^m(t) = \begin{bmatrix} \boldsymbol{x}_s(t) \\ \boldsymbol{x}^f(t) \end{bmatrix}, \quad \dot{\boldsymbol{\xi}}(t) = \begin{bmatrix} \dot{\xi}_s(t) \\ \dot{\xi}_n(t) \end{bmatrix}.$$

Equivalent discrete-time description of sampled system is:

$$\boldsymbol{x}_{i+1}^m = \boldsymbol{F}^m \boldsymbol{x}_i^m + \boldsymbol{w}_i^m, \tag{40}$$

$$z_i = \boldsymbol{d}^{m\prime} \boldsymbol{x}_i^m, \tag{41}$$

Similarly to (25) $\boldsymbol{w}_i^m$ is a zero mean vector Gaussian noise with $\mathrm{E}\{\boldsymbol{w}_i^m \boldsymbol{w}_i^{m\prime}\} = \boldsymbol{W}^m$,

$$\boldsymbol{W}^m = \int_0^h \mathrm{e}^{\boldsymbol{A}^m s} \boldsymbol{C}^m \boldsymbol{C}^{m\prime} \mathrm{e}^{\boldsymbol{A}^{m\prime} s} \, ds \quad \text{and} \quad \boldsymbol{F}^m = \mathrm{e}^{\boldsymbol{A}^m \tau}, \tag{42}$$

vectors $\boldsymbol{x}_0^m$ and $[\boldsymbol{w}_i^{m\prime}, n_i]$ are independent for all $i \geq 0$.

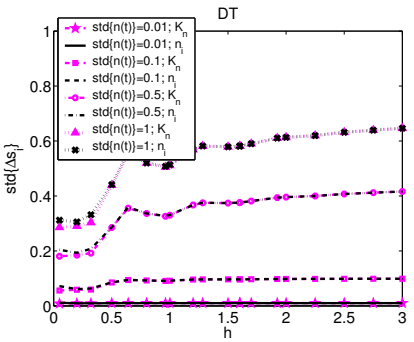

Fig. 5. Comparison of exact and approximate DT Kalman filter

3.3 Discrete-time model

While appropriate for continuous-time signal processing modeling, the model in (30)–(32) is completely inadequate for discrete-time models. This is because sampling of physically nonexisting continuous-time white noise with infinite variance can not be defined reasonable.

Therefore we propose a discrete-time model of instantaneously sampled noisy signal

$$\boldsymbol{x}^s_{i+1} = \boldsymbol{F}_s \boldsymbol{x}^s_i + \boldsymbol{w}^s_i, \tag{43}$$

$$z_i = \boldsymbol{d}'_s \boldsymbol{x}^s_i + n_i, \tag{44}$$

$$s_i = \boldsymbol{d}'_s \boldsymbol{x}^s_i \tag{45}$$

in which noise is presented as discrete-time white noise n_i whose variance ρ^2 equals to the variance of $n(t)$ of the original system, i.e. $\rho^2 = \mathrm{var}\{n_i\} = \mathrm{var}\{n(t)\}$, and can be calculated as

$$\rho^2 = \boldsymbol{d}'_n \boldsymbol{Q}_n \boldsymbol{d}_n, \tag{46}$$

where $\boldsymbol{Q}_n$ fulfills the following Lyapunov equation:

$$\boldsymbol{A}_n \boldsymbol{Q}_n + \boldsymbol{Q}_n \boldsymbol{A}'_n = -\boldsymbol{d}_n \boldsymbol{d}'_n \tag{47}$$

and

$$\boldsymbol{F}_s = \mathrm{e}^{\boldsymbol{A}_s h}, \ \boldsymbol{W}_s = \int_0^h \mathrm{e}^{\boldsymbol{A}_s v} \boldsymbol{c}_s \boldsymbol{c}'_s \mathrm{e}^{\boldsymbol{A}'_s v} \, dv \tag{48}$$

To find the estimate $\hat{s}_i = E\{s_i | z_i\}$ classical discrete Kalman filter is used in the following form:

$$\hat{\boldsymbol{x}}_{i+1|i+1} = \boldsymbol{F}_s \hat{\boldsymbol{x}}_{i|i} + \boldsymbol{k}^f (z_{i+1} - \boldsymbol{d}'_s \boldsymbol{F}_s \hat{\boldsymbol{x}}_{i|i}), \tag{49}$$

$$\boldsymbol{k}^f = \frac{\boldsymbol{\Sigma} \boldsymbol{d}_s}{\boldsymbol{d}'_s \boldsymbol{\Sigma} \boldsymbol{d}_s + \rho^2}, \tag{50}$$

$$\boldsymbol{\Sigma} = \boldsymbol{W}_s + \boldsymbol{F}_s \left(\boldsymbol{\Sigma} - \frac{\boldsymbol{\Sigma} \boldsymbol{d}_s \boldsymbol{d}'_s \boldsymbol{\Sigma}'}{\boldsymbol{d}'_s \boldsymbol{\Sigma} \boldsymbol{d}_s + \rho^2} \right) \boldsymbol{F}'_s. \tag{51}$$

Again, since only a rough characterization of noise is required, and filter equations are of lower order, this greatly simplifies discrete-time filtering.

A comparison between exact and approximate Kalman filter for the exemplary system is shown in Fig. 5. Again, there is very little to choose between them except perhaps for short sampling periods h.

4. SAMPLING QUALITY ASSESSMENT

The quality of sampling will be measured by their standard deviations from the actual values. Denote $\Delta s^*(i)$ the difference between actual value s_i and a sample z_i, and

$$\Delta s^*(i) = s_i - z_i = \boldsymbol{d}^{o\prime}_s \boldsymbol{x}_i + \boldsymbol{d}^{o\prime} \boldsymbol{x}_i. \tag{52}$$

and $\sigma^2(\Delta s^*) = \lim_{i \to \infty} \mathrm{var}\{\Delta s^*(i)\}$ the corresponding variance, and $\sigma^2(\Delta s)$ the difference between s_i and its estimate $\hat{s}_{i|i}$ produced by the discrete-time Kalman filter,

$$\Delta s(i) = s_i - \hat{s}_{i|i} = \boldsymbol{d}^{o\prime}_s \boldsymbol{x}_i - \boldsymbol{d}^{m\prime}_s \hat{\boldsymbol{x}}_{i|i}), \tag{53}$$

with corresponding variance $\sigma^2(\Delta s) = \lim_{i \to \infty} \mathrm{var}\{\Delta s(i)\}$.

We then have

$$\sigma^2(\Delta s) = \boldsymbol{d}^{o\prime}_s \boldsymbol{V}^o \boldsymbol{d}^o_s - 2 \cdot \boldsymbol{d}^{o\prime}_s \boldsymbol{V}^{of} \boldsymbol{d}^m_s + \boldsymbol{d}^{m\prime}_s \boldsymbol{V}^f \boldsymbol{d}^m_s, \tag{54}$$

$$\sigma^2(\Delta s^*) = \boldsymbol{d}^{o\prime}_s \boldsymbol{V}^o \boldsymbol{d}^o_s - 2 \cdot \boldsymbol{d}^{o\prime}_s \boldsymbol{V}^o \boldsymbol{d}^o + \boldsymbol{d}^{o\prime} \boldsymbol{V}^o \boldsymbol{d}^o, \tag{55}$$

with:

$$\boldsymbol{V} = \boldsymbol{\Lambda} \boldsymbol{V} \boldsymbol{\Lambda}' + \boldsymbol{\Gamma} \boldsymbol{W}^o \boldsymbol{\Gamma}' + \boldsymbol{\Phi} \boldsymbol{\Phi}' \nu^{o2}, \tag{56}$$

(ν^{o2}=0 is mostly assumed in the paper) where:

$$\boldsymbol{\Lambda} = \begin{bmatrix} \boldsymbol{F}^o & \boldsymbol{0} \\ \boldsymbol{k}^f_i \boldsymbol{d}^{o\prime} \boldsymbol{F}^o & \boldsymbol{F}^m - \boldsymbol{k}^f_i \boldsymbol{d}^{m\prime} \boldsymbol{F}^m \end{bmatrix},$$

$$\boldsymbol{\Gamma} = \begin{bmatrix} \boldsymbol{I}^o \\ \boldsymbol{k}^f_i \boldsymbol{d}^{o\prime} \end{bmatrix}, \ \boldsymbol{\Phi} = \begin{bmatrix} \boldsymbol{0} \\ \boldsymbol{k}^f_i \end{bmatrix}, \ \boldsymbol{V} = \begin{bmatrix} \boldsymbol{V}^o & \boldsymbol{V}^{f,o} \\ \boldsymbol{V}^{f,o} & \boldsymbol{V}^f \end{bmatrix}.$$

5. PROPERTIES OF SAMPLING AND FILTERING SYSTEMS

We will study the properties of various combinations of continuous-time and discrete-time filters as displayed in Fig. 6 for an exemplary system defined by

$$K_s(s) = \frac{1}{(1+3s)^2}, \quad K_n(s) = \frac{k_n}{T_n^2 s^2 + 2\zeta_n T_n s + 1} \tag{57}$$

$$T_n = 0.1, \quad \zeta_n = 0.2, \tag{58}$$

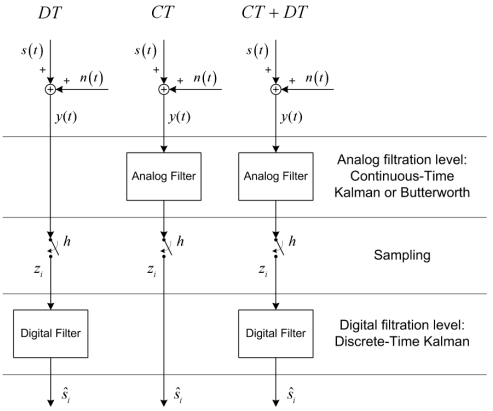

Fig. 6. Configurations of filters and samplers. CT – continuous-time; DT – discrete-time

5.1 Continuous-time filters: frequency domain analysis

The spectral density of the continuous-time process $y(t)$ as well as that of discrete-time samples $y(ih)$ for different sampling periods and k_n choosen so that $\mathrm{var}\{n(t)\} = 1$ are shown in Fig. 1.

In Fig. 2 the spectral density of $y(t)$ is compared with spectral densities of processes on outputs from analog filters: a Kalman and an anti-aliasing Butterworth 2-nd order ones determined for different sampling periods h. An important observation is that, as one might expect,

the anti-aliasing filter does not change $S_c^f(\omega)$ for small ω while the Kalman filter does. The latter does not support the intuition standing behind the idea of anti-aliasing. It is also interesting that the spectral densities of both filtered signals do not differ from their sampled counterparts in a wide range of frequencies, see Fig. 7

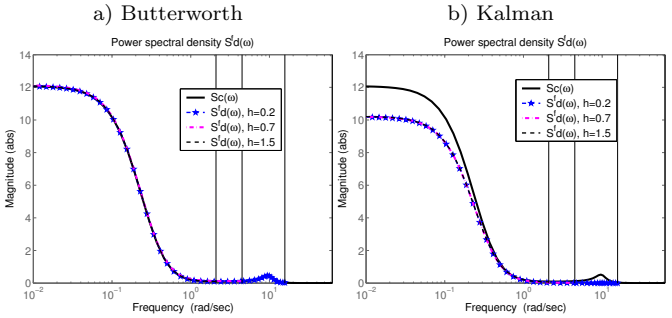

Fig. 7. Continuous and discrete power spectral densities plotted only up to Nyquist frequency

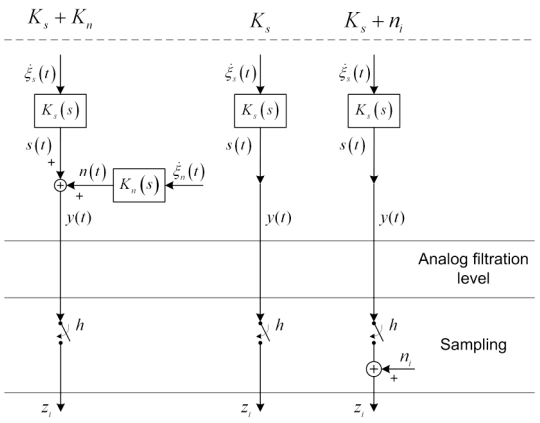

Fig. 8. Models for purely discrete Kalman filter design

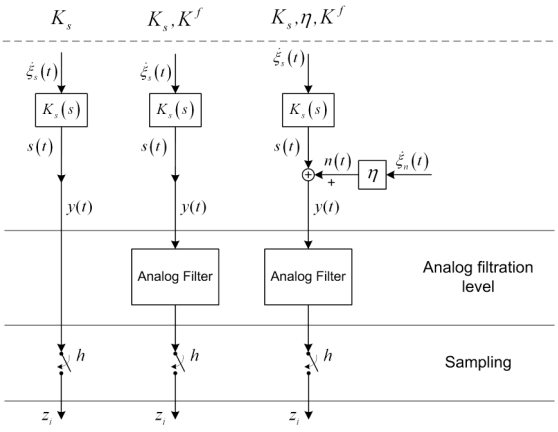

Fig. 9. Models of analog path for discrete Kalman filter design

5.2 Discrete-time filters

Purely discrete-time filters In order to design a discrete-time Kalman filter working on samples from the observed signal $y(t)$ a model of that signal is necessary. Models under consideration are displayed in Fig. 8. From left to right we have a full model marked $K_s + K_n$, a model completetly neglecting noise marked K_s, and a model marked $K_s + n_i$ in which noise is represented as a discrete-time white noise added to the sampler.

Discrete-time filters following continuous-time filters When the output from a continuous-time filter is sampled we consider three typical situations depicted in Fig. 9. The first one, marked K_s neglects existence of both filter and noise, the second marked K^f takes the transfer function $K^f(s)$ of the filter into account neglecting noise, and finally, the third approximates the colored noise with continuous-time white noise.

5.3 Comparison of results

There are three groups of plots in Fig. 10 showing the properties of various filtering and sampling variants for three different values of sampling period h. We compare the results of pure discrete-time Kalman filter, continuous-time Kalman filter and anti-aliasing Butterworth filter, and a combination of anti-aliasing filter followed by a discrete-time Kalman filter designed under various assumptions concerning the continuous-time filter output model.

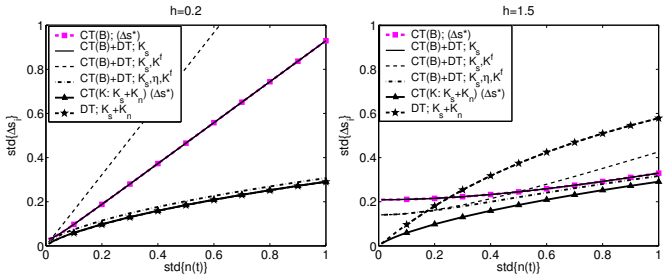

Fig. 10. Comparison of different structures

As one might expect the best results are obtained when process $y(t)$ is filtered with a continuous-time Kalman filter before being sampled, and the accuracy of results does not depend on sampling frequency. This result can be considered the lower bound for achievable accuracy.

For small sampling periods, the purely discrete-time Kalman filter working on rough samples behaves as good as the continuous-time one but, as one might expect with increasing sampling period its quality decreases.

It is interesting to note that the quality of anti-aliasing filter at high sampling rates is rather poor and increases at longer sampling periods and not too small magnitudes of noise.

The sampled output from the anti-aliasing filter can be further improved using an appropriately designed discrete-time Kalman filter. The best results are obtained for the model of continuous-time part consisting of the model of signal, filter and noise. We used here the simplified model with continuous-time white noise.

The results are much worse when the model of the filter output does not contain any model of noise. It is surprising that even better results are obtained when the model of filter is omitted. The former is exactly what is suggested in

the literature, for example in the control context: apply an anti-aliasing filter, add its transfer function to the transfer function of the plant and forget about noise, or even about the disturbance.

Another interesting perspective to study the results is provided by plots being functions of h with parameter $\rho = \mathrm{std}\{n(t)\}$, see Fig. 11–Fig. 12.

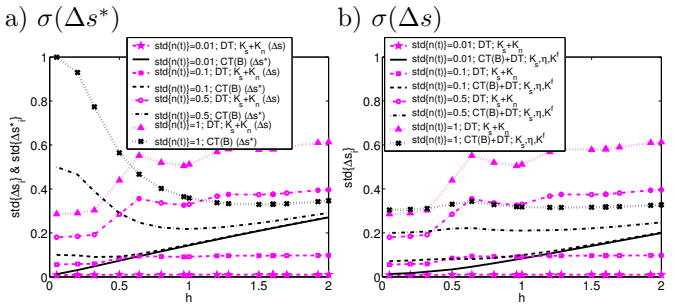

Fig. 11. a) Butterworth vs DT Kalman b) Butterworth +DT Kalman vs DT Kalman alone

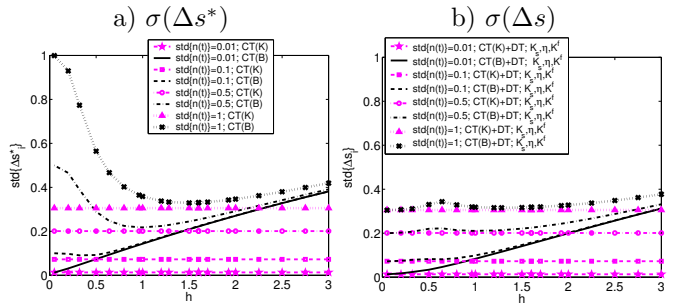

Fig. 12. a) Butterworth vs CT Kalman b) Butterworth+DT Kalman vs CT Kalman, $0 < h \leq 3$

Realizations of filtered output processes, as well as results of discrete-time Kalman filtering of their samples are depicted in Fig. 13–Fig. 14

6. CONCLUSION

The range of reasonable sampling periods for anti-aliasing sampling is rather small, and stretches around optimal value that depends on the noise level. Augmenting the sampler with a discrete Kalman filter improves the results for smaller sampling periods bringing the filtration error close to the lower limit provided by an analog Kalman filter. It does however almost not help for sampling periods greater than optimal. Small noise level results in a small value of optimal sampling period which makes averaging sampling useless.

The best solution is to employ an analog Kalman filter to filter the signal before being sampled, or a discrete-time Kalman filter at sampling rate high enough. In the latter case the result can be further re-sampled if a reduction of sampling rate is necessary. Simplified noise models contribute to accurate enough and simple filters, both analog and discrete.

REFERENCES

B.D.O. Anderson and J.B. Moore. *Optimal Filtering.* Prentice Hall, Inc., Englewood Cliffs, New Jersey, 1979.

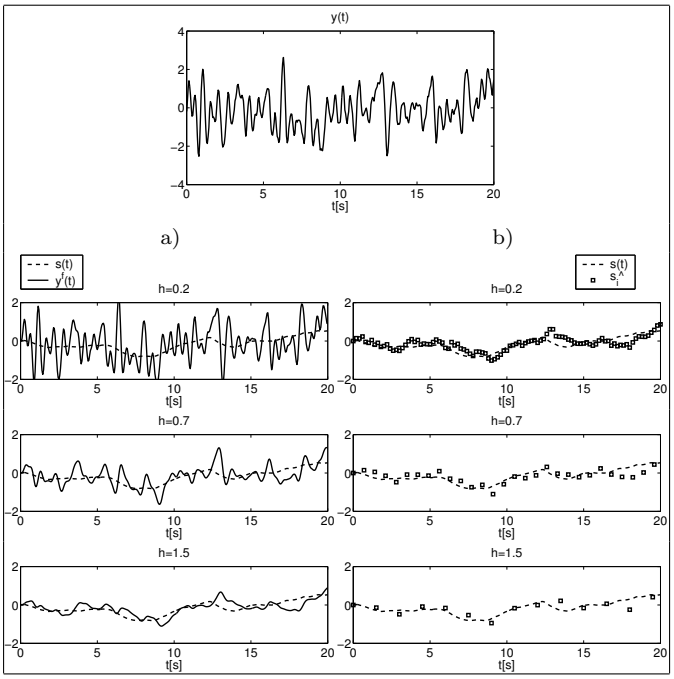

Fig. 13. Realizations for $\mathrm{std}\{n(t)\} = 1$: a) CT(B) b) CT(B)+DT; K_s, K_n, K^f.

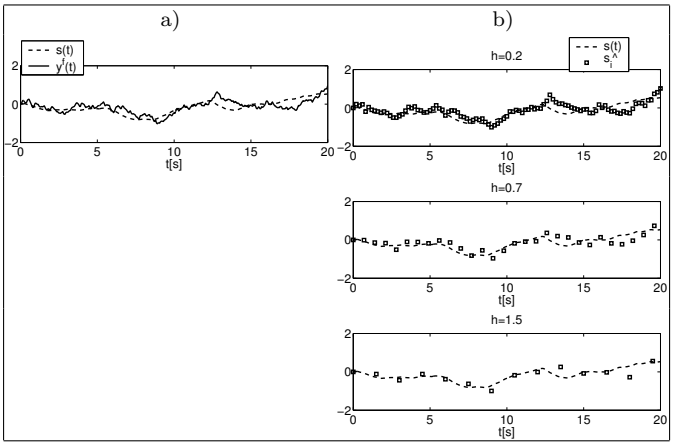

Fig. 14. Realizations for $\mathrm{std}\{n(t)\} = 1$: a) CT(K:K_s, K_n) b) CT(K:K_s, K_n)+DT; K_s, K_n, K^f. ($y(t)$ is the same as in Fig. 13)

K. Åström and B. Wittenmark. *Computer–Controlled Systems.* Prentice Hall, 1997.

A. Feuer and G. Goodwin. *Sampling in Digital Signal Processing and Control.* Birkhäuser Boston, 1996.

A.J. Jerri The Shannon sampling theorem - its variuos extensions and applications: a tutorial review. Proc. IEEE vol. 65, pp. 1656–1596, 1977

B. Wittenmark, K. J. Åström and K-E Årzén. *Computer Control: An Overview.* IFAC Professional Brief, January 2002.